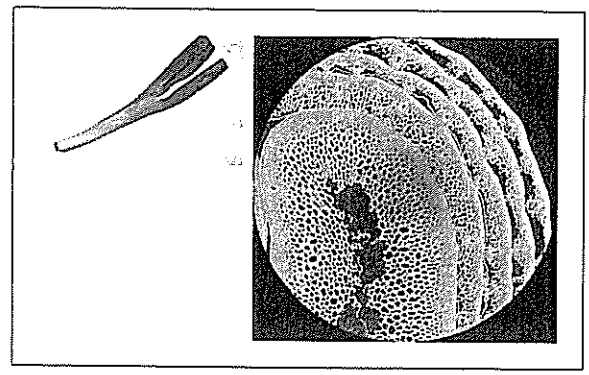

図10　顕微鏡CTによるネギの画像

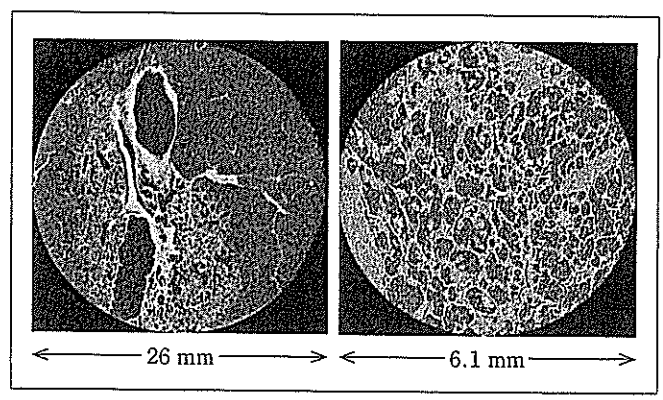

図11　肺がんの顕微鏡CT像

き，「いかに早期にがんを見つけるか」についての研究を行っています。そこでは，実際に検診を行って，がん検診の精度についての評価を行っています。表1は，センター設立の2004年2月から2005年1月までの1年間での，3,792名の方を検診させていただいた結果ですが，なんとそのうちの5%の方でがんが見つかっています。受診者の年齢などの理由もあるかも知れませんが，医療者としては，まだまだがんがあるのにそれが発見されないでいる人たちが，世の中に多いのではないか，という不安を強くおぼえる結果です。

がんの早期発見，がん検診については，診断器機についてもどんどん新しいものが開発されていますので，そのいくつかをご紹介します。

“CT（Computer Tomography）”という言葉もかなり一般的となりましたが，それがさらに進んだものに「ヘリカルCT」があります。「ヘリカル」というのは「らせん」という意味で，受診者のからだの回りをグルグル回ることで，より細密に画像データを収集できます。その結果，普通のレントゲンでは分か

表2 がんに負けないための秘訣

1. 生活習慣に気をつけましょう。
2. 検診を受けて早期発見，早期治療。
3. がんになったら，自分のがんの勉強をしましょう。
4. 担当医の話を良く聞き，分からないところは質問しましょう。
5. そして納得の行く治療を受けましょう。

らないような小さながんを見つけることや，そのデータをコンピュータで計算し，肺なら肺の立体的な画像（3D画像）を作ることも可能になります。図9は検診にCTを導入する前と後での，発見された肺がん患者の生存率を比較したものですが，大きな差が出ています。これはすなわち，治療で治すことができるような小さな肺がん，早期の肺がんがCTで発見されたことによります。

さらにCTは発展しており，「顕微鏡CT」というものも登場しました。がんを治療する上で，そのがんの性格，組織型を知ることが重要なのですが，そのためには実際に患者さんのがんの細胞を採って診断する必要があります。病巣に針を刺すようなことが必要ですから，患者さんにとって大きな苦痛となる検査です。顕微鏡CTは，そうした問題をクリアすべく研究が進められているものです。図10は，皆さんがイメージしやすいように，ネギを顕微鏡CTで撮影したものです。図11は肺の組織で，左は約10倍，右は約30倍程度の拡大像です。図左では，正常な肺では空気が入っているところ（肺胞）はつぶれていない一方，がんの部位ではそれが硬くなってしまい，がん細胞が周囲に浸潤していることが分かります。図右では，肺胞の中に向かってがんが増殖していることが分かります。こうした技術がさらに進歩すると，肺に針を刺し組織を採る，というような検査が不要になるのではないかと考えています。

おわりに～がんに負けないための秘訣

最後に私が考える「がんに負けないための秘訣」を表2にまとめました。

まず「生活習慣に気をつけよう」。がんは生活習慣病であり，とくに喫煙ががん発生原因の1/3を占めることも皆さんよくご存じだと思います。黄緑色野菜をたくさん取るなど，普段の生活で健康に気をつけましょう。

そして「検診を受けて早期発見，早期治療」。今日のお話でその意義は十分

ご理解いただけたと思います。

がんという病気になってしまったら，「自分のがんについて勉強をしましょう」。そして「担当医の話をよく聞き，分からないことは質問しましょう」。その上で自分で考え，「納得いく治療を受けましょう」。

これが本日の皆さまへの最後のメッセージです。築地の国立がんセンターの周囲には，素晴らしいところがたくさんあります。お時間があったら，どうぞ見学においでください。

【参考資料】

〔資料 1〕財団法人がん研究振興財団：がんとどう付き合うか「大腸がん」予防と診断・治療・社会復帰と緩和ケア.

〔資料 2〕厚生省がん研究助成金，厚生省がん克服 10 か年戦略：がん—厚生科学の挑戦.

【シリーズ『がん医療の現在』バックナンバーから】

今回の講演では，さまざまな分野についてお話しましたが，各テーマについてさらに詳しく知りたい方は，本講演会シリーズの記録である『がん医療の現在（いま）』（医事出版社）のバックナンバーをご参照ください。以下に，近刊を中心に，今回のテーマにかかわる主なものを挙げておきます。

◎ がん発生のメカニズムについて：

- 廣橋説雄「がん研究の現状と展望」，がん医療の現在 No. 11（2004 年）所収.〔資料 3〕
- 若林敬二「がんの発生要因と予防方法」，がん医療の現在 No. 13（2005 年）所収.〔資料 4〕

◎ 内視鏡的治療について：

- 齊藤大三「消化管がん（食道がん・胃がん・大腸がん）の内視鏡的治療」，がん医療の現在 No. 10（2004 年）所収.

◎ 化学療法，分子標的治療薬について：

- 西尾和人「がんの分子標的治療～新しいがん治療の開発動向」，がん医療の現在 No. 9（2003 年）所収.
- 田村友秀「がんの化学療法（抗がん剤による治療）～肺がんを中心に」，がん医療の現在 No. 14（2006 年）所収.

◎ 免疫療法について：

- 高上洋一「がんの免疫療法と造血幹細胞移植」，がん医療の現在 No. 12（2005 年）所収.

◎ がん検診について：

- 祖父江友孝「がん予防・検診の最新情報～どのような検診をどのように受けるべきか」，がん医療の現在 No. 12（2005 年）所収.
- 森山紀之「がん検診でどこまでわかるか～がん予防・検診研究センターの役わりとPET」，がん医療の現在 No. 14（2006 年）所収.

Q “PET”の検診精度はいかがでしょうか。

A “PET”については，前回（第19回）の本市民公開講演会で，予防・検診センター長の森山先生が詳しくお話されましたので今回は触れませんでした。PETでのがんの発見率は，やはりがんの進行度や種類などに影響されます。本日は肺のヘリカルCTについてご説明しましたが，たとえばごくごく早期の肺がんについては，PETよりヘリカルCTのほうが検診精度は高いということは言えます。しかし，診断精度の「評価」は，必ずしも「より小さいがんが見つかること」でなされるのではなく，「そのがんが見つかることで治療成績が改善されること」にあります。ですから，仮に肺がんに対するPETの診断精度がヘリカルCTに劣ったとしても，それでも十分治療が可能である程度に精度が高ければ，PET検査を受ければそれで十分である，という判断もできます。

診断技術の進歩によって，以前では考えられないくらい小さながんが見つかるようになってきましたが，果たしてそれが間違いなく生命に危険を及ぼすようながんにまで進行するのか，ひょっとしたら消えてしまうものもあるのではないか，という問いに対して十分回答できるほどのデータが現時点ではないのです。危険性の少ないがんを治療することで，患者さんに余計な侵襲を加えてしまう可能性も否定できません。ですから，予防・検診研究センターではそうしたデータをたくさん集め，研究しているのです。

PETはオールラウンドな検査であり，その利用価値は計り知れないものがあります。PETで見つからないがんがあるということが，すなわちPETが不要であるという結論にはなりません。

Q 日本のがん医療も，世界の流れである放射線治療をもっと進める努力が必要ではないかと思います。

A ご指摘の通り，日本のがん医療は外科が優勢で，その他の治療法が少し遅れをとっているところはあります。国，行政のレベルでも，現在，放射線の治療専門医を何とかして増やそうと努力しています。先ほど池田先生も触れられましたが，各施設の放射線治療の管理が精度高く行われているのかを第三者的視点からチェックするような試みもその一環と言え，もう少し時間をいただければ，放射線治療もどんどん普及していくのではないかと思っています。そのように放射線治療の力の認識が広まっていけば，若い医師もそれに刺激され，高いモチベーション，インセンティブをもってその専門医を目指す人も増えていくと思います。放射線治療に限らず，化学療法等にしても，これから専門医をどんどん増やしていかなければなりません。

（編集部注：今回の講演の主旨と異なる質疑応答については割愛させていただきました。）

ANTICANCER RESEARCH *26*: 3317-3326 (2006)

Local Delivery of Doxorubicin for Malignant Glioma by a Biodegradable PLGA Polymer Sheet

YOSHINOBU MANOME[1], TOSHIAKI KOBAYASHI[2], MARIKO MORI[3], RIE SUZUKI[1], NAOTAKE FUNAMIZU[1], NOBUTAKE AKIYAMA[4], SACHIKO INOUE[5], YASUHIKO TABATA[5] and MICHIKO WATANABE[1]

Departments of [1]Molecular Cell Biology, [3]Pathology and [4]Molecular Immunology, Jikei University School of Medicine, 3-25-8 Nishishinbashi, Minato-ku, Tokyo, 105-8461; [2]Cancer Screening Technology Division, Research Center for Cancer Prevention and Screening, National Cancer Center, 5-1-1 Tsukiji, Chuo-ku, Tokyo, 105-0045; [5]Department of Biomaterials, Institute for Frontier Medical Sciences, Kyoto University, 53 Kawara-cho Shogoin, Sakyo-ku, Kyoto 606-8507, Japan

Abstract. *Implantable, biocompatible and biodegradable devices bearing an anticancer drug can provide promising local therapy to patients with malignant disorders. With the aim of treating brain tumors, especially gliomas, a membranous sheet containing doxorubicin was produced by co-polymerization to poly(D,L-lactide-co-glycolide) (PLGA). When release of the drug from the sheet was measured, sustained release continued until day 34. The data contrasted with the burst release from material containing a higher proportion of the drug. In terms of biodegradability, a subcutaneous 3 x 3-mm tetragonal sheet was almost completely absorbed by day 80. When a glioma was implanted subcuteneously and the tumor nodule exposed to the sheet, the device inhibited tumor growth significantly. The sheet consisted of an amorphous structure with cavities estimated to have a diameter of 0.5 – 3 μm by electron microscopic observation. Since the sheet is implantable, biodegradable and has a sustained-drug release property, the device may play a role in the local therapy of brain tumors.*

Malignant brain tumor, such as infiltrating glioma and glioblastoma, is one of the most intractable diseases in the human body. The invasive character and rapid proliferation of the cells often brings recurrence of the disease even after radical treatment and an increase in intracranial hypertension eventually causes herniation due to limited intracranial space. The median survival time is 0.4 years for glioblastoma and is 5.6 years even for more benign low-grade astrocytoma (1). Most patients die within 2 to 5 years after their diagnosis. In spite of recent advances in radiotherapy, immunotherapy, chemotherapy and other adjuvant therapies, the prognosis has not been dramatically improved and more effective therapies are required. Although the prognosis is poor, the tumors seldom metastasize to regions outside of the central nervous system. In addition, the main etiology of death is local recurrence. Therefore, if local recurrence can be prevented, long-term survival or even a complete cure of the patient can be expected.

The main problem of administering chemotherapy for malignancy in the central nervous system is the low efficiency of drug delivery to the residual tumor in brain parenchyma. When anti-malignant drugs are systemically administered, most drugs may not reach the lesion due mainly to the existence of the blood-brain barrier. From the aspect of chemotherapy, alkylating agents such as temozolomide and nitrosourea represented by ACNU or BCNU are the first choice of drugs in combination with radiation (2, 3). These drugs are potent against malignant gliomas since they can cross the blood-brain barrier and enter the tumor cells. They confer toxicity even to not-actively dividing cells, which account for approximately 70% of the brain tumor (4). Moreover, alkylating agents can synchronize cells in the G2M phase and, thus, function as radiosensitizers when combined with therapeutic irradiation. Regardless of such a promising efficacy of the drug, the prognosis of patients has not improved sufficiently. The reason is partly attributable to the low local drug concentration, because the drug delivery is not adequate in spite of penetrability of the drug through the blood-brain barrier (5, 6). When these facts are considered, it is obvious that the development of more potent local treatment is required.

Correspondence to: Yoshinobu Manome, MD, Ph.D., Department of Molecular Cell Biology, Institute of DNA Medicine, Jikei University School of Medicine, Japan. Tel: +81-3-3433-1111 Ext. 2360, Fax: +81-45-628-4757, e-mail: manome@jikei.ac.jp

Key Words: Doxorubicin, PLGA, local delivery, glioma.

0250-7005/2006 $2.00+.40

Recent advances in material engineering have provided a new material for such local treatment. One representative example is the BCNU-loaded PLGA wafer (7). PLGA is a biodegradable and biocompatible material, and the BCNU-loaded PLGA wafer is an implantable polymeric device that releases BCNU directly into the tumor tissue. Implanting the device after surgery can eliminate the residual tumor tissue in the operative field and delay recurrence. The antitumor activity of the wafer has been demonstrated (8, 9) and the device might be useful because most patients with glioma undergo surgical removal and chemotherapy as well as radiotherapy.

However, there is a concern about alkylating agent-based local chemotherapy, because tumor cells soon acquire resistance after the systemic administration of drugs. The mechanism of resistance is mainly *via* the recruitment of O_6-methylguanin merthyltransferase, a DNA repair enzyme into tumor cells (10-13). MGMT facilitates stoichiometric transfer of the O_6-alkyl groups from the alkylated DNA molecules to its own cysteine residues and by so doing, is itself deactivated after acceptance of the alkyl groups. Overexpression of MGMT repairs the DNA damage caused by the alkylating agents. Chemotherapeutic agents, such as temozolomide and nitrosourea, induce MGMT expression in the tumor cells and resistance may influence the effect of focal treatment with the BCNU wafer. In such cases, treatment with another anti-malignant drug with a different mechanism of action might be useful. Based on this concept doxorubicin was selected.

The mechanism of doxorubicin resistance is expression of the multiple drug resistant gene (MDR); moreover, it does not show cross-resistance to alkylating agents. In addition, doxorubicin has been used commonly in patients with disseminated lymphoma or leukemia in the cerebrospinal fluid by intrathecal injection and its safety has been well recognized. Thus, doxorubicin was co-polymerized to biodegradable PLGA and a membrane containing the drug was developed. Ultimately, the possibility of modulating the glioma after surgery using the membrane could be explored.

Materials and Methods

Doxorubicin sheet. Doxorubicin hydrochloride ((2S,4S)-4-(3-amino-2,3,6-trideoxy-α-L-*lyxo*-hexopyranosyloxy)-1,2,3,4-tetrahydro-2,5,12-trihydroxy-2-hydroxyacetyl-7-methoxynaphthacene-6,11-dione monohydrochloride; DOX or Adriamycin) was provided by Kyowa Hakko Kogyo Co. Ltd. (Tokyo, Japan). One square centimeter of the sheet contained 1 mg of doxorubicin. To prepare an 8.4 cm^2 surface of the sheet, 8.4 mg of doxorubicin were mixed with 318 mg of PLGA (50:50 molar ratio, Mw53114) dissolved in chloroform. The mixture was co-polymerized by the solvent-evaporation method and used after further desiccation.

Release of doxorubicin in vitro. Measurement of the drug concentration in the solvent was determined by the UV-2200A spectrophotometer (Shimadzu, Kyoto, Japan). The doxorubicin sheet was set under physiological conditions for days (pH7.4, 37°C in phosphate-buffered saline) and the total amount of the eluted doxorubicin was quantified.

Animal experiments. To investigate the biodegradation of the doxorubicin sheet, closed colony Jcl:ICR mice were purchased from Clea Japan, Tokyo and bred in a standard animal facility. For the tumor implantation and treatment study, five-week old Fischer 344 rats were purchased from Sankyo Laboratory, Tokyo, Japan. These animals were maintained under conditions of 28°C and 55-60% humidity and given free access to food and tap water. All the animal procedures were performed under the guidance of the committee in the animal care facility. In the first set of animal experiments, the 3 x 3 mm tetragon sheet was subcutaneously implanted into the left flank of an ICR mouse. After implantation, absorption of the sheet was determined by weighing the unabsorbed residuals after removal. Degradability was expressed as a percentile of the original sheet weight on the day of observation (n=5 in each group). In the second set of the experiment, the RT2 glioma cell line, syngeneic to the Fischer 344 rat, was used. The RT2 glioma cells were cultured in Dulbecco's minimum essential medium supplemented with 10% bovine serum (GIBCO Laboratories, Grand Island, NY, USA). Three x 10^5 of the trypsinized and dispersed cells in 100 μl of PBS were subcutaneously injected into the rat's right flank and four days later, after confirmation of establishment of the tumor nodule, the rats were treated with 2.1125 cm^2 of doxorubicin sheet containing 2.1 mg of doxorubicin by covering the tumor. For some animals, 8.4 mg/100 μl of doxorubicin were directly injected into the center of the tumor. Tumor volumes were measured and growth was directly accessed. Statistical analysis was performed by the two-tailed Student's *t*-test.

Morphological examination of the doxorubicin sheet by electron microscopy. For the scanning electron microscopy, the doxorubicin sheet was lightly washed in water then fixed with 1.2% glutaraldehyde in 0.1 M phospate-buffered saline then adjusted to pH 7.4. The specimen was dehydrated by ascending concentrations of ethanol and the critical point drying method using liquid CO_2. After the dehydration, the sample was coated with ion-sputtered gold and palladium and observed by a JSM-5800LV Scanning Electron Microscope (JEOL Ltd., Tokyo, Japan) at the accelerating voltage of 15 KV. For transmission electron microscopy, the sheet was fixed with 2% glutaraldehyde in phosphate-buffer and the specimens were subjected to examination by an H-7500 Electron Microscope (Hitachi, Tokyo, Japan) at the accelerating voltage of 100 KV.

Results

Release of doxorubicin from the doxorubicin sheet. The release of doxorubicin from the PLGA membrane was first determined *in vitro*. The concentration of doxorubicin was measured by absorption spectrophotometric analysis. The absorbance of light by doxorubicin in continuous wavelength was measured by a spectrophotometer (Figure 1A) and the correlation of both 232 nm and 480 nm peaks for determination of the doxorubicin concentration was confirmed. The amount of drug in the solvent was

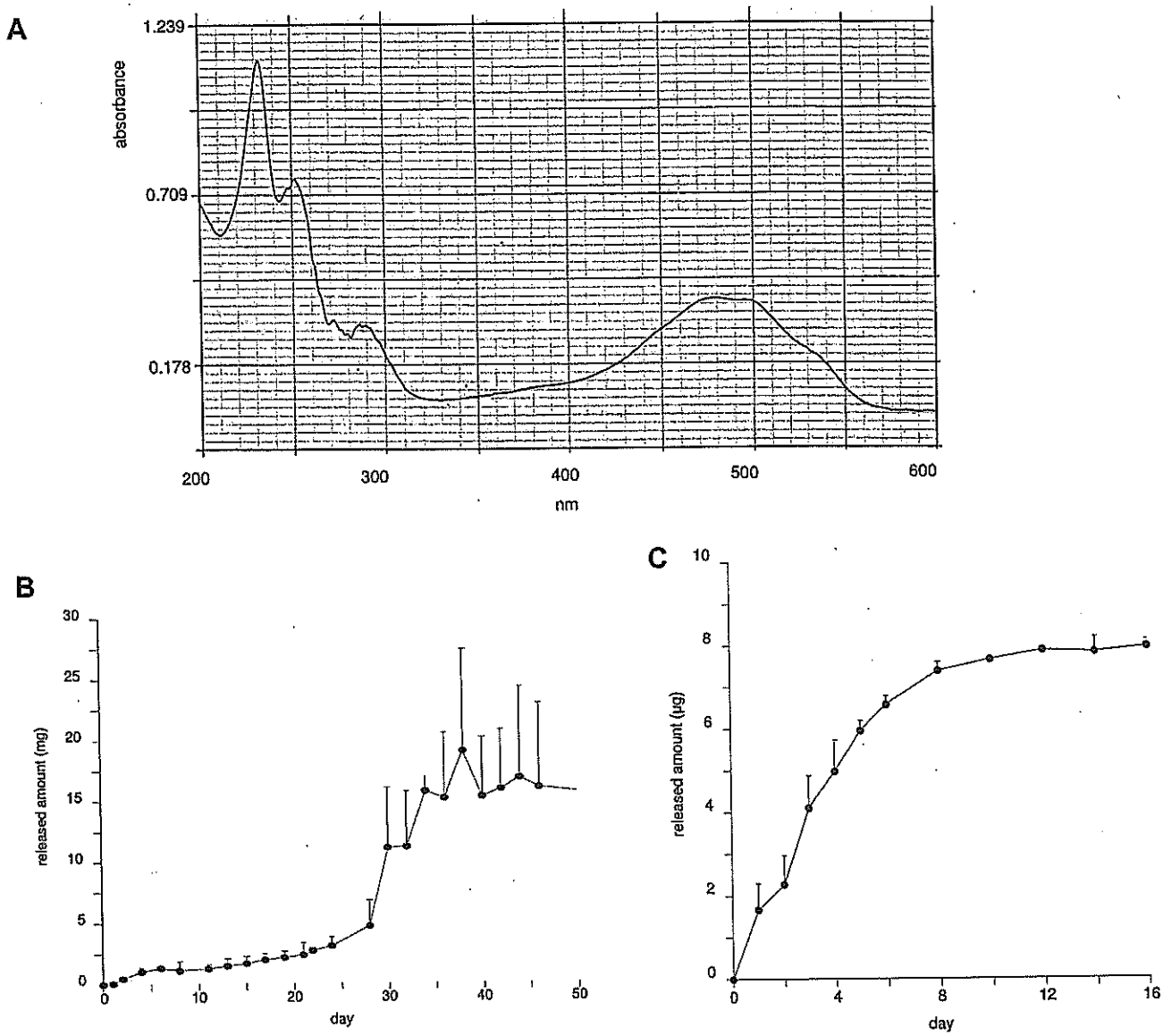

Figure 1. *Release of doxorubicin from the sheet in vitro. A) Spectrophotometric properties of doxorubicin. The light absorbance of doxorubicin was measured by continuous change in the wave length. Based on the figure, the absorbances at 232 nm and 480 nm were used for further determination of the drug concentration. Values measured at both peaks correlated well with drug concentrations. B) Total amount of doxorubicin released from 1 mg of the sheet. Release gradually started from immediately after the exposure and 10% of the drug was released by day 10. The sheet steadily discharged the drug and sustained release continued until day 28. After the burst release around day 30 to 34, further release was not detected. The result is expressed as the mean of two experiments; bars, S.D. C) Release from the drug-overloaded sheet. When the drug concentration was increased 3-fold when co-polymerized to PLGA, the sheet released the drug much faster than the ordinary sheet. Most of the drug was released by day 8 and further release was not prominent after day 10. The result is expressed as the mean of two experiments; bars, S.D.*

quantified at the 480-nm wavelength. The PLGA sheet containing doxorubicin was left under physiological conditions and the total amounts of doxorubicin released were measured (Figure 1B). Release started from day 1 and gradually increased until day 24. Subsequently, the release was abruptly increased and continued until day 34. Thirty-four days after the experiment, the release reached a peak. The released amount was followed up until day 178, however further release was not detected in the experiment (data not shown). The pattern of slow release from the sheet might derive from the proportions of doxorubicin and PLGA. When the load of doxorubicin was increased in the sheet, a three-fold higher drug discharge occurred at an earlier stage of the experiment (Figure 1C). The drug burst

started from the day of the experiment and most of the doxorubicin was released by day 8. Unlike the previous result, sustained release was not detected in this drug-enriched sheet. The sheet did not retain doxorubicin after 12 days of experiments.

Biodegradation of the sheet in mice. Since deliberate release of the drug from the sheet was demonstrated *in vitro*, the biodegradability of the sheet was examined next. After implantation of the sheet into the left flank of the mice, changes in the dry-weight of the sheet were measured and recorded chronologically. The sheet degraded according to the passage of time. Degradation rapidly progressed in the initial stage and continued until day 78. The sheet was ultimately absorbed. It took more than 80 days to disappear and further changes in weight could not be determined. During the process, the doxorubicin sheet was assimilated and other than pigmentation in the adjacent area, caused

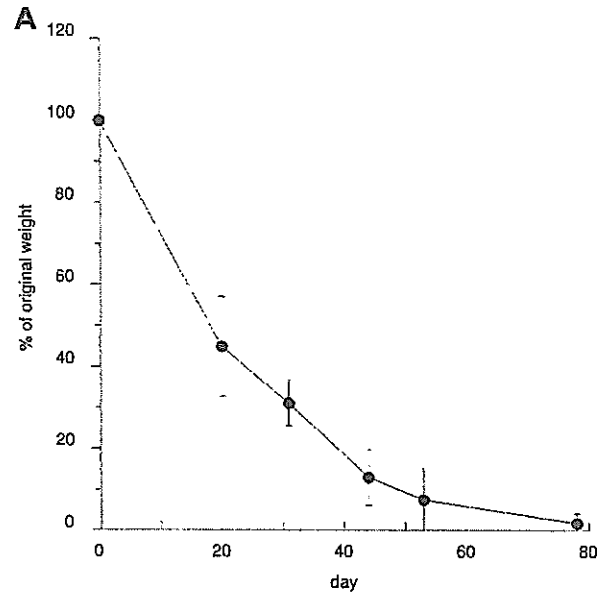

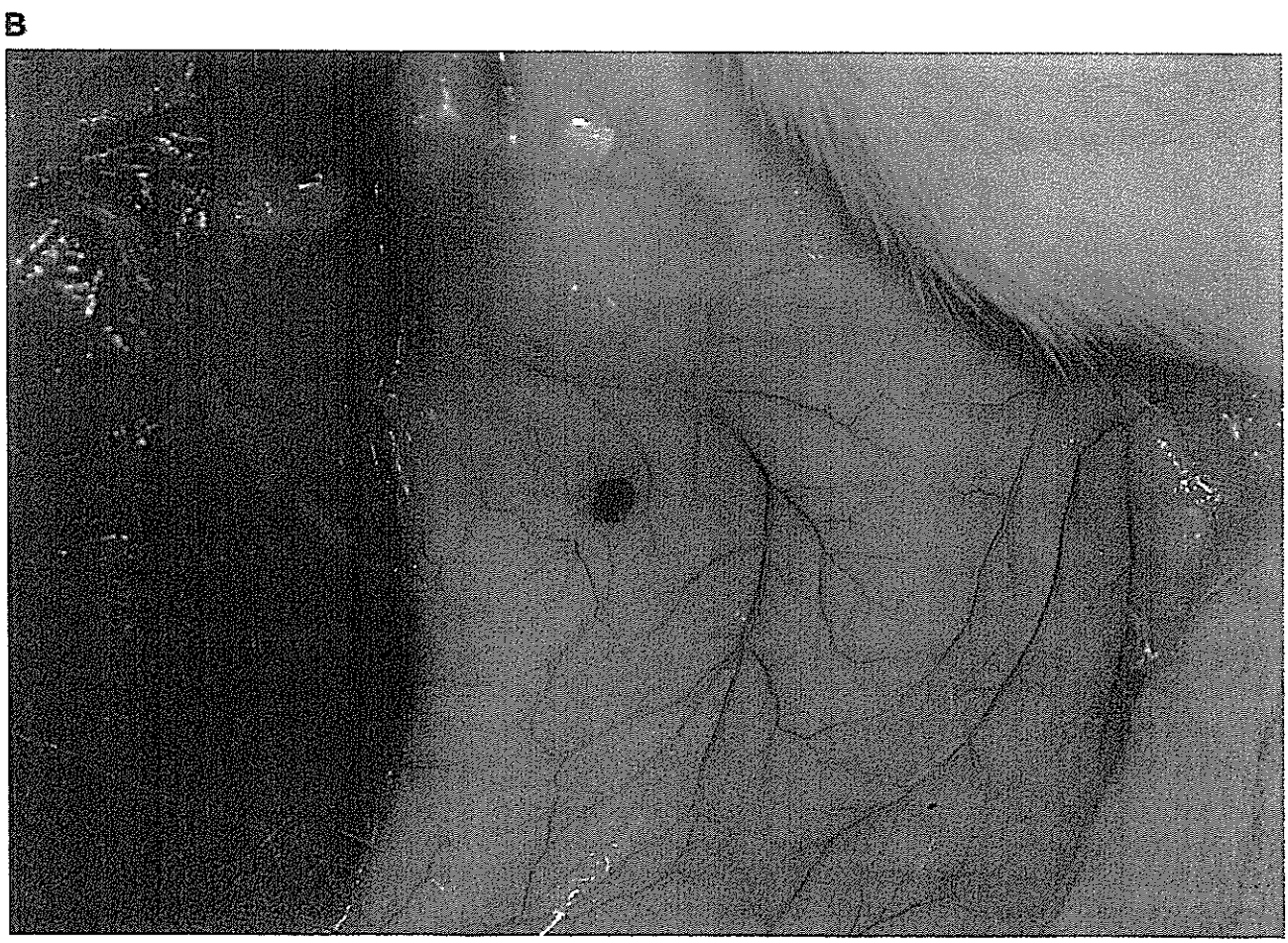

Figure 2. *Biodegradability of the sheet in vivo. A) The dry-weight of the implanted sheet was measured and biodegradability was expressed as a percentage of the original weight. The sheet degraded according to the passage of time. There was a rapid decrease in volume from the start of the experiment, followed by gradual degradation. More than 78 days were required for complete absorption. The result is expressed as the mean of five animals at each time point; bars, S.D. B) Biodegradability of the subcutaneously implanted sheet. The picture shows the sheets at 52 days after implantation. The sheet was degraded, but still visible with a change in the color of the surrounding subcutaneous tissue. Pigmentation of tissue occurred in the contact area of the sheet.*

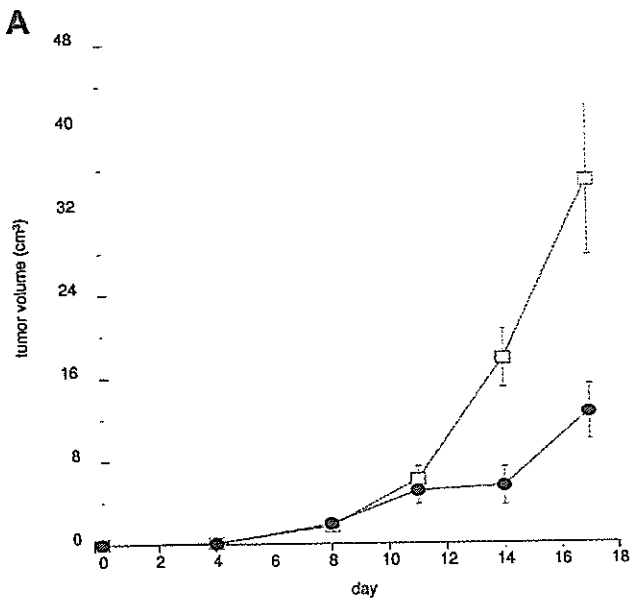

neither inflammation nor substantial necrosis in the surrounding tissue (Figure 2A, B).

Effect of the released doxorubicin on the established tumor. The slow-release character and biodegradability of the sheet enables potential application of the sheet for tumor treatment *in vivo*. In the final examination, the sheet was used for the treatment of subcutaneously implanted RT2 syngeneic malignant glioma tumor cells. After growth, the tumor was covered with a doxorubicin sheet and the subsequent growth was measured. Tumors treated with a mock sheet increased in size exponentially (Figure 3). In contrast, growth of the tumor was inhibited in rats treated with the doxorubicin sheet. On the 17th day of the experiment, the tumor volume reached more than 30 cm^3 and the rats started to die in the control group, whereas the group treated with the doxorubicin sheet exhibited a smaller tumor size. There were inter-group differences in volumes

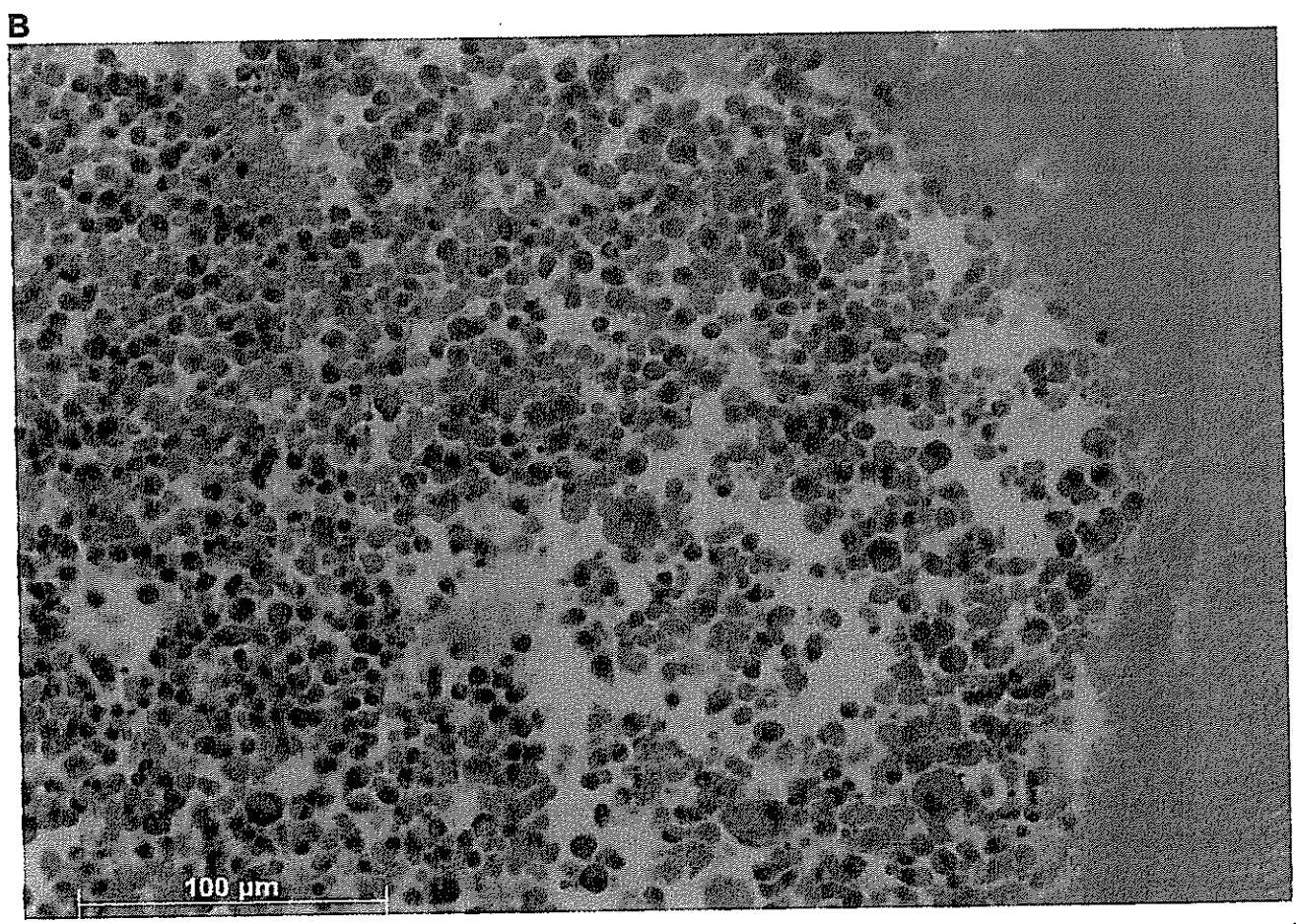

Figure 3. *Tumor growth inhibition by the sheet. A) After glioma cells were implanted, the tumor nodule was treated to the sheet. While tumors in control animals grew prosperously, treatment inhibited the expansion of the tumor. Mock sheet treatment (□); doxorubicin sheet treatment (●). There were differences on day 14 (p=0.064) and day 17 (p=0.019). The result was demonstrated as a mean of five animals in each group; bars, S.D. B) Histology of tumor cells with the sheet (on day 17, hematoxylin-eosin staining). Tumor tissue or cells (left) adjoining the sheet (right) were necrotic with erythrocytes.*

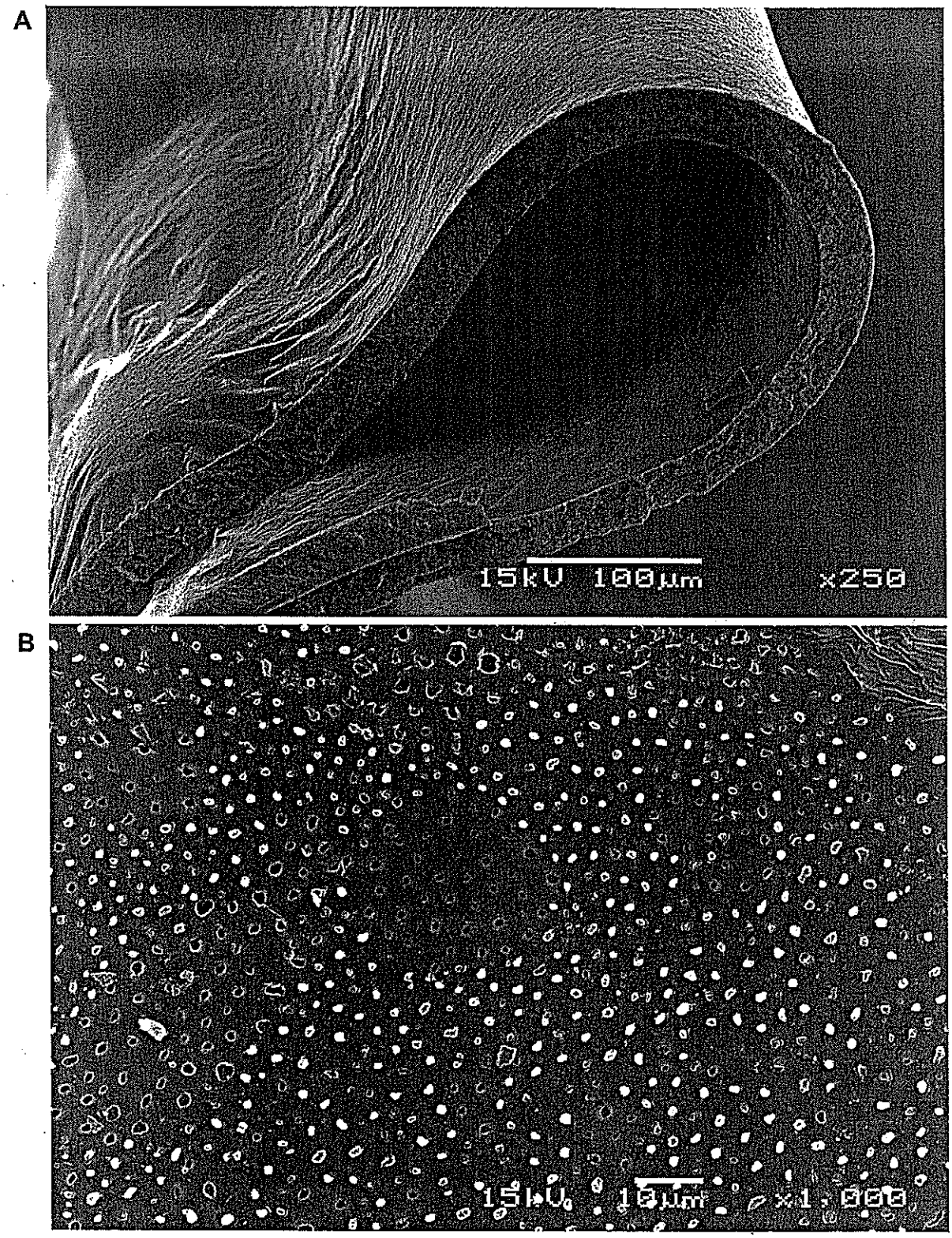

Figure 4. *Ultrastructure of doxorubicin sheet by electron microscopy. A-C) Pictures taken by scanning electron microscope, D) By transmission electron microscope. A) Overview: the sheet had a flexible texture with a thickness of 10 µm. B) Surface: the surface consisted of amorphous material with small holes. Grains of the drug resided in these small holes with a diameter of 0.5 to 3 µm. C) Vertical section (ethanol-cracked surface): after fixation, the sample was ethanol-cracked in liquid nitrogen. Cross-section disclosed the porous structure of the membrane sheet. D) Cross-section of the sheet: the drug was encircled by an amorphous electro-density substrate. Direct magnification, x15000.*

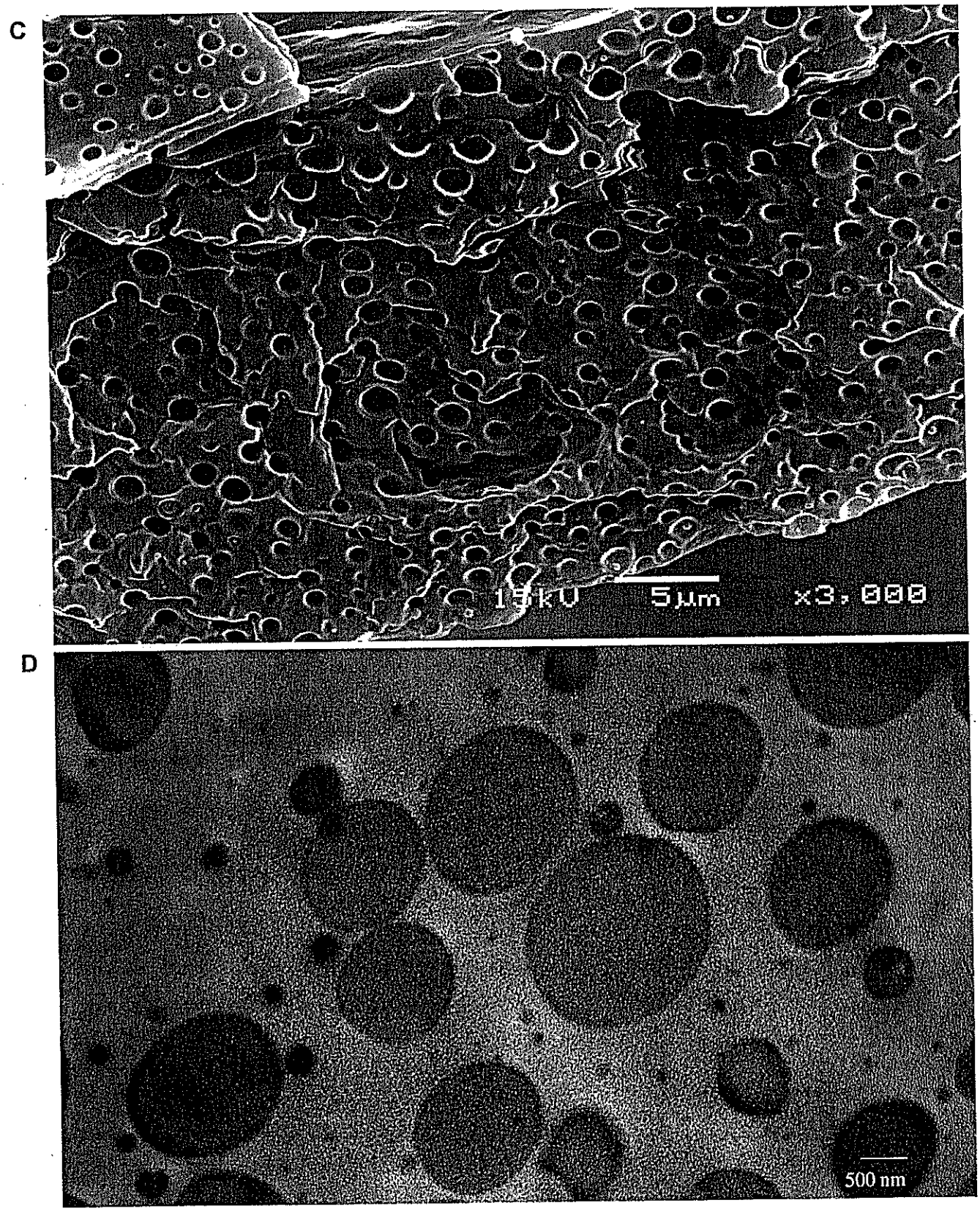

Figure 4. *continued*

on days 14 and 17 (p=0.064 and 0.019, respectively). The sizes of tumors treated with the doxorubicin sheet were comparable to those of animals treated by direct injection with a 4-times higher total dose (on day 14: injection 4.88±2.33 cm^3 *vs.* sheet 5.50±1.81 cm^3, on day 17: 14.80±6.62 cm^3 *vs.* 12.56±2.65 cm^3).

Morphological studies of the sheet. The sheet's ability to confer toxicity to the target tumor by releasing the drug was confirmed. To further investigate the material, the sheet was examined by electronmicroscopy. The sheet had a thickness of 10 μm and was flexible (Figure 4A). The surface of the sheet consisted of an amorphous structure with small cavities having a diameter of 0.5 to 3 μm. A grain, presumably of drug, was held in each cavity and some of these protruded to the surface. Some of the cavities were empty, but this may have been due to elution of the drug during preparation of the specimen (Figure 4B). An ethanol-cracked, vertical section revealed the spongy, cheese-like structure of the sheet. Most of the cavity was hollow due to the same reason as above, but the drug is visible in the cavities through a small exit (Figure 4C). This finding was confirmed by transmission electronmicroscopy (Figure 4D). The structure of the sheet may be responsible for sustained release of the drug.

Discussion

In this study, a doxorubicin-loaded poly (D, L-lactide-co-glycolide) membrane was developed and drug release from the membrane, biodegradation and efficacy on implanted glioma cells were examined.

As a scaffold for drug polymerization, PLGA was chosen. Similar to other polymers (14), PLGA has been used, not only as biodegradable polyester elastomers in tissue engineering (15), but also as a carrier of drugs, antigens, or genes either by itself or in combination with other appropriate materials. Owing to its safety, performance, cost and ease-of-use, this material was especially useful as a drug delivery tool for anticancer drugs. Micro- or nano-particles of PLGA conjugates include paclitaxel (16-20), doxorubicin (21-23), floxuridine (24), cystatins (25), camptothetin (26), 5-fluorouracil (27, 28), oxaliplatin (29), methotrexate (30) and cisplatin (31). In addition to the anticancer agents, tumor antigen (32, 33), photodynamic (34-37) or radiosensitizer (38, 39), genes (40-42) or DNA decoys (43), anti-angiogenic agents (44, 45), usnic acid (46), interferons (47), immunotoxin (48), all-trans retinoic acid (49), hormones (42, 50) and other compounds have been conjugated to PLGA for the treatment of malignant diseases.

Nano- or micro-particles of PLGA have drug delivery advantages, such as achievement of a higher concentration in the target tissue, sustained release and a longer circulation time in plasma as well as lower toxicity. However, from the stand-point of brain tumor therapy, especially considering the prevention of recurrence, there is an advantage of local therapy with an implantable drug-conjugated device, even though diffusion of nanoparticles is relatively limited to the vicinity of the implantation site (27). Accordingly, a wafer with BCNU was successfully developed (7, 8, 51). In other solid tumors, local treatment with PLGA polymers with paclitaxel and vinca alkaloid were developed and tested in clinical pilot trials (52, 53).

We chose doxorubicin for co-polymerization to PLGA. This drug has a long history and has been used widely for the treatment of malignancies, including leukemias, lymphomas and many solid tumors, including brain tumors. Accordingly, its pharmacokinetics are well known. From the aspect of safety, the drug can be administrated intrathecally with few serious adverse effects (54, 55). This might compromise safety if leakage of the drug occurs into the cerebrospinal fluid. Moreover, resistance to alkylating agent due mainly to overexpression of MGMT generally does not demonstrate cross-resistance to doxorubicin, which blocks DNA and RNA synthesis by inhibiting topoisomerase II. The sheet might be especially useful for patients with recurrent drug-resistant gliomas initially treated by alkylating agents.

Local therapies are key options for the treatment of brain tumors. BCNU-loaded wafers and other implantable nano- and micro-particles are the materials of first choice. It is preferable to increase the number of effective devices or drugs for local treatment. Since our PLGA-based sheet is implantable, easy to prepare, wholly degradable and displays a sustained-release property, it may play a role in the treatment for malignant brain tumors as a local therapy device.

Acknowledgements

The work was partly supported by a Grant-in-Aid for the Third Term Comprehensive Control Research for Cancer. We thank Hideki Saito, Emi Kikuchi and Yuko Abe in the Jikei University School of Medicine, Japan, for skillful technical assistances.

References

1 Ohgaki H and Kleihues P: Population-based studies on incidence, survival rates, and genetic alterations in astrocytic and oligodendroglial gliomas. J Neuropathol Exp Neurol *64*: 479-489, 2005.

2 Barrie M, Couprie C, Dufour H, Figarella-Branger D, Muracciole X, Hoang-Xuan K, Braguer D, Martin PM, Peragut JC, Grisoli F and Chinot O: Temozolomide in combination with BCNU before and after radiotherapy in patients with inoperable newly diagnosed glioblastoma multiforme. Ann Oncol *16*: 1177-1184, 2005.

3 Cohen MH, Johnson JR and Pazdur R: Food and Drug Administration Drug approval summary: temozolomide plus radiation therapy for the treatment of newly diagnosed glioblastoma multiforme. Clin Cancer Res *11*: 6767-6771, 2005.

4 Yoshii Y, Maki Y, Tsuboi K, Tomono Y, Nakagawa K and Hoshino T: Estimation of growth fraction with bromodeoxyuridine in human central nervous system tumors. J Neurosurg *65*: 659-663, 1986.

5 Hamstra DA, Moffat BA, Hall DE, Young JM, Desmond TJ, Carter J, Pietronigro D, Frey KA, Rehemtulla A and Ross BD: Intratumoral injection of BCNU in ethanol (DTI-015) results in enhanced delivery to tumor – a pharmacokinetic study. J Neurooncol *73*: 225-238, 2005.

6 Yimam MA, Bui T and Ho RJ: Effects of lipid association on lomustine (CCNU) administered intracerebrally to syngeneic 36B-10 rat brain tumors. Cancer Lett, 2006.

7 Seong H, An TK, Khang G, Choi SU, Lee CO and Lee HB: BCNU-loaded poly(D, L-lactide-co-glycolide) wafer and antitumor activity against XF-498 human CNS tumor cells *in vitro*. Int J Pharm *251*: 1-12, 2003.

8 Lee JS, An TK, Chae GS, Jeong JK, Cho SH, Lee HB and Khang G: Evaluation of *in vitro* and *in vivo* antitumor activity of BCNU-loaded PLGA wafer against 9L gliosarcoma. Eur J Pharm Biopharm *59*: 169-175, 2005.

9 Westphal M, Hilt DC, Bortey E, Delavault P, Olivares R, Warnke PC, Whittle IR, Jaaskelainen J and Ram Z: A phase 3 trial of local chemotherapy with biodegradable carmustine (BCNU) wafers (Gliadel wafers) in patients with primary malignant glioma. Neuro-oncol *5*: 79-88, 2003.

10 Bobola MS, Silber JR, Ellenbogen RG, Geyer JR, Blank A and Goff RD: O6-methylguanine-DNA methyltransferase, O_6-benzylguanine, and resistance to clinical alkylators in pediatric primary brain tumor cell lines. Clin Cancer Res *11*: 2747-2755, 2005.

11 Hermisson M, Klumpp A, Wick W, Wischhusen J, Nagel G, Roos W, Kaina B and Weller M: O_6-methylguanine DNA methyltransferase and p53 status predict temozolomide sensitivity in human malignant glioma cells. J Neurochem *96*: 766-776, 2006.

12 Manome Y, Watanabe M, Futaki K, Ishiguro H, Iwagami S, Noda K, Dobashi H, Ochiai Y, Ohara Y, Sanuki K, Kunieda T and Ohno T: Development of a syngenic brain-tumor model resistant to chloroethyl-nitrosourea using a methylguanine DNA methyltransferase cDNA. Anticancer Res *19*: 5313-5318, 1999.

13 Manome Y, Yoshinaga H, Watanabe M and Ohno T: Adenoviral transfer of antisenses or ribozyme to O_6-methylguanine-DNA methyltransferase mRNA in brain-tumor model resistant to chloroethyl-nitrosourea. Anticancer Res *22*: 2029-2036, 2002.

14 Lesniak MS, Upadhyay U, Goodwin R, Tyler B and Brem H: Local delivery of doxorubicin for the treatment of malignant brain tumors in rats. Anticancer Res *25*: 3825-3831, 2005.

15 Webb AR, Yang J and Ameer GA: Biodegradable polyester elastomers in tissue engineering. Expert Opin Biol Ther *4*: 801-812, 2004.

16 Fonseca C, Simões S and Gaspar R: Paclitaxel-loaded PLGA nanoparticles: preparation, physicochemical characterization and *in vitro* anti-tumoral activity. J Control Release *83*: 273-286, 2002.

17 Kang BK, Chon SK, Kim SH, Jeong S, Kim MS, Cho SH, Lee HB and Khang G: Controlled release of paclitaxel from microemulsion containing PLGA and evaluation of anti-tumor activity *in vitro* and *in vivo*. Int J Pharm *286*: 147-156, 2004.

18 Mo Y and Lim LY: Paclitaxel-loaded PLGA nanoparticles: potentiation of anticancer activity by surface conjugation with wheat germ agglutinin. J Control Release *108*: 244-262, 2005.

19 Mo Y and Lim LY: Preparation and *in vitro* anticancer activity of wheat germ agglutinin (WGA)-conjugated PLGA nanoparticles loaded with paclitaxel and isopropyl myristate. J Control Release. *107*: 30-42, 2005.

20 Sahoo SK and Labhasetwar V: Enhanced antiproliferative activity of transferrin-conjugated paclitaxel-loaded nanoparticles is mediated *via* sustained intracellular drug retention. Mol Pharm *2*: 373-383, 2005.

21 Lin R, Shi Ng L and Wang CH: *In vitro* study of anticancer drug doxorubicin in PLGA-based microparticles. Biomaterials *26*: 4476-4485, 2005.

22 Yoo HS and Park TG: Biodegradable polymeric micelles composed of doxorubicin conjugated PLGA-PEG block copolymer. J Control Release *70*: 63-70, 2001.

23 Mallery SR, Pei P, Kang J, Ness GM, Ortiz R, Touhalisky JE and Schwendeman SP: Controlled-release of doxorubicin from poly(lactide-co-glycolide) microspheres significantly enhances cytotoxicity against cultured AIDS-related Kaposi's sarcoma cells. Anticancer Res *20*: 2817-2825, 2000.

24 Inoue K, Onishi H, Kato Y, Michiura T, Nakai K, Sato M, Yamamichi K, Machida Y and Nakane Y: Comparison of intraperitoneal continuous infusion of floxuridine and bolus administration in a peritoneal gastric cancer xenograft model. Cancer Chemother Pharmacol *53*: 415-422, 2004.

25 Cegnar M, Premzl A, Zavasnik-Bergant V, Kristl J and Kos J: Poly(lactide-co-glycolide) nanoparticles as a carrier system for delivering cysteine protease inhibitor cystatin into tumor cells. Exp Cell Res *301*: 223-231, 2004.

26 Tong W, Wang L and D'Souza MJ: Evaluation of PLGA microspheres as delivery system for antitumor agent-camptothecin. Drug Dev Ind Pharm *29*: 745-756, 2003.

27 Roullin VG, Deverre JR, Lemaire L, Hindre F, Venier-Julienne MC, Vienet R and Benoit JP: Anti-cancer drug diffusion within living rat brain tissue: an experimental study using [^{3}H](6)-5-fluorouracil-loaded PLGA microspheres. Eur J Pharm Biopharm *53*: 293-299, 2002.

28 Hagiwara A, Sakakura C, Shirasu M, Yamasaki J, Togawa T, Takahashi T, Muranishi S, Hyon S and Ikada Y: Therapeutic effects of 5-fluorouracil microspheres on peritoneal carcinomatosis induced by Colon 26 or B-16 melanoma in mice. Anticancer Drugs *9*: 287-289, 1998.

29 Lagarce F, Cruaud O, Deuschel C, Bayssas M, Griffon-Etienne G and Benoit J: Oxaliplatin loaded PLAGA microspheres: design of specific release profiles. Int J Pharm *242*: 243-246, 2002.

30 Singh UV and Udupa N: *In vitro* characterization of methotrexate loaded poly(lactic-co-glycolic) acid microspheres and antitumor efficacy in Sarcoma-180 mice bearing tumor. Pharm Acta Helv *72*: 165-173, 1997.

31 Kumagai S, Sugiyama T, Nishida T, Ushijima K and Yakushiji M: Improvement of intraperitoneal chemotherapy for rat ovarian cancer using cisplatin-containing microspheres. Jpn J Cancer Res *87*: 412-417, 1996.

32 Waeckerle-Men Y and Groettrup M: PLGA microspheres for improved antigen delivery to dendritic cells as cellular vaccines. Adv Drug Deliv Rev *57*: 475-482, 2005.

33 Waeckerle-Men Y, Scandella E, Uetz-Von Allmen E, Ludewig B, Gillessen S, Merkle HP, Gander B and Groettrup M: Phenotype and functional analysis of human monocyte-derived dendritic cells loaded with biodegradable poly(lactide-co-glycolide) microspheres for immunotherapy. J Immunol Methods *287*: 109-124, 2004.

34 McCarthy JR, Perez JM, Bruckner C and Weissleder R: Polymeric nanoparticle preparation that eradicates tumors. Nano Lett *5*: 2552-2556, 2005.

35 Vargas A, Pegaz B, Debefve E, Konan-Kouakou Y, Lange N, Ballini JP, van den Bergh H, Gurny R and Delie F: Improved photodynamic activity of porphyrin loaded into nanoparticles: an *in vivo* evaluation using chick embryos. Int J Pharm *286*: 131-145, 2004.

36 Konan YN, Berton M, Gurny R and Allemann E: Enhanced photodynamic activity of meso-tetra(4-hydroxyphenyl)porphyrin by incorporation into sub-200 nm nanoparticles. Eur J Pharm Sci *18*: 241-249, 2003.

37 Konan YN, Chevallier J, Gurny R and Allemann E: Encapsulation of p-THPP into nanoparticles: cellular uptake, subcellular localization and effect of serum on photodynamic activity. Photochem Photobiol *77*: 638-644, 2003.

38 Geze A, Venier-Julienne MC, Saulnier P, Varlet P, Daumas-Duport C, Devauchelle P and Benoit JP: Modulated release of IdUrd from poly (D,L-lactide-co-glycolide) microspheres by addition of poly (D,L-lactide) oligomers. J Control Release *58*: 311-322, 1999.

39 Reza MS and Whateley TL: Iodo-2'-deoxyuridine (IUdR) and 125IUdR loaded biodegradable microspheres for controlled delivery to the brain. J Microencapsul *15*: 789-801, 1998.

40 Prabha S and Labhasetwar V: Critical determinants in PLGA/PLA nanoparticle-mediated gene expression. Pharm Res *21*: 354-364, 2004.

41 Jilek S, Ulrich M, Merkle HP and Walter E: Composition and surface charge of DNA-loaded microparticles determine maturation and cytokine secretion in human dendritic cells. Pharm Res *21*: 1240-1247, 2004.

42 Panyam J, Zhou WZ, Prabha S, Sahoo SK and Labhasetwar V: Rapid endo-lysosomal escape of poly(DL-lactide-co-glycolide) nanoparticles: implications for drug and gene delivery. Faseb J *16*: 1217-1226, 2002.

43 Gill JS, Zhu X, Moore MJ, Lu L, Yaszemski MJ and Windebank AJ: Effects of NFkappaB decoy oligonucleotides released from biodegradable polymer microparticles on a glioblastoma cell line. Biomaterials *23*: 2773-2781, 2002.

44 Benny O, Duvshani-Eshet M, Cargioli T, Bello L, Bikfalvi A, Carroll RS and Machluf M: Continuous delivery of endogenous inhibitors from poly(lactic-co-glycolic acid) polymeric microspheres inhibits glioma tumor growth. Clin Cancer Res *11*: 768-776, 2005.

45 Bandi N, Ayalasomayajula SP, Dhanda DS, Iwakawa J, Cheng PW and Kompella UB: Intratracheal budesonide-poly(lactide-co-glycolide) microparticles reduce oxidative stress, VEGF expression, and vascular leakage in a benzo(a)pyrene-fed mouse model. J Pharm Pharmacol *57*: 851-860, 2005.

46 Ribeiro-Costa RM, Alves AJ, Santos NP, Nascimento SC, Goncalves EC, Silva NH, Honda NK and Santos-Magalhaes NS: *In vitro* and *in vivo* properties of usnic acid encapsulated into PLGA-microspheres. J Microencapsul *21*: 371-384, 2004.

47 Sanchez A, Tobio M, Gonzalez L, Fabra A and Alonso MJ: Biodegradable micro- and nanoparticles as long-term delivery vehicles for interferon-alpha. Eur J Pharm Sci *18*: 221-229, 2003.

48 Ferdous AJ, Stembridge NY and Singh M: Role of monensin PLGA polymer nanoparticles and liposomes as potentiator of ricin A immunotoxins *in vitro*. J Control Release *50*: 71-78, 1998.

49 Jeong YI, Song JG, Kang SS, Ryu HH, Lee YH, Choi C, Shin BA, Kim KK, Ahn KY and Jung S: Preparation of poly(DL-lactide-co-glycolide) microspheres encapsulating all-trans retinoic acid. Int J Pharm *259*: 79-91, 2003.

50 Labrie F, Li S, Belanger A, Cote J, Merand Y and Lepage M: Controlled release low dose medroxyprogesterone acetate (MPA) inhibits the development of mammary tumors induced by dimethyl-benz(a) anthracene in the rat. Breast Cancer Res Treat *26*: 253-265, 1993.

51 Chae GS, Lee JS, Kim SH, Seo KS, Kim MS, Lee HB and Khang G: Enhancement of the stability of BCNU using self-emulsifying drug delivery systems (SEDDS) and *in vitro* antitumor activity of self-emulsified BCNU-loaded PLGA wafer. Int J Pharm 301: 6-14, 2005.

52 Rohr UD, Oberhoff C, Markmann S, Gerber B, Scheulen M and Schindler AE: The safety of synthetic paclitaxel by intralesional delivery with OncoGeltrade mark into skin breast cancer metastases: method and results of a clinical pilot trial. Arch Gynecol Obstet 1-7, 2005.

53 Fournier C, Hecquet B, Bouffard P, Vert M, Caty A, Vilain MO, Vanseymortier L, Merle S, Krikorian A, Lefebvre JL *et al*: Experimental studies and preliminary clinical trial of vinorelbine-loaded polymeric bioresorbable implants for the local treatment of solid tumors. Cancer Res *51*: 5384-5391, 1991.

54 Jordan B, Pasquier Y and Schnider A: Neurological improvement and rehabilitation potential following toxic myelopathy due to intrathecal injection of doxorubicin. Spinal Cord *42*: 371-373, 2004.

55 Arico M, Nespoli L, Porta F, Caselli D, Raiteri E and Burgio GR: Severe acute encephalopathy following inadvertent intrathecal doxorubicin administration. Med Pediatr Oncol *18*: 261-263, 1990.

Received May 5, 2006
Accepted May 29, 2006

Neurol Med Chir (Tokyo) 46, 169–175, 2006

Three-Way Bipolar Forceps: A Novel Bipolar Coagulator System for Nerve Stimulation and Detection of Nerve Potentials

Yoshiyuki FUJITA*, Yoshihiro MURAGAKI*,**, Kyojiro NAMBU*, Tomokatsu HORI**, and Hiroshi ISEKI*,**

*Faculty of Advanced Techno-surgery, Institute of Advanced Biomedical Engineering and Science, Graduate School of Medicine, and **Department of Neurosurgery, Neurological Institute, Tokyo Women's Medical University, Tokyo

Abstract

Preoperative characterization of brain anatomy by magnetic resonance imaging and intraoperative functional characterization of the nervous system is essential in patients undergoing radical resection of brain tumors. A novel integrated system was developed combining conventional bipolar forceps with an electric stimulator and an oscilloscope. The system consists of a mechanical switching circuit allowing a wide range of electric characteristics and was designed to perform intraoperative electrophysiological studies, including functional mapping and measurements of motor evoked potentials (MEPs) and somatosensory evoked potentials (SEPs). This system achieved a significant reduction in exchange time (from 3.63 ± 1.00 sec to 1.12 ± 0.42 sec) between coagulation and stimulation, and reproducible measurement of MEPs from porcine limbs by cortical stimulation using the bipolar forceps. Functional mapping under awake craniotomy was carried out by cortical stimulation in patients with glioblastoma, and median nerve SEPs with high signal-to-noise ratio were elicited from the bipolar forceps on the sensory cortex of patients under general anesthesia. This integrated system is technically easy to operate and allows functional monitoring of an area that would otherwise be difficult to access using conventional methods. This three-way bipolar forceps system may reduce postoperative complications in patients undergoing neurosurgical procedures.

Key words: bipolar forceps, intraoperative monitoring, functional mapping, somatosensory evoked potential, motor evoked potential

Introduction

Functional monitoring of neurological activity using electrophysiological techniques is essential to reduce functional compromise during resection or coagulation of tumors involving the central nervous system. Such techniques include functional mapping by intraoperative electrical stimulation during awake surgery to identify the speech and motor areas,[10] motor evoked potential (MEP) monitoring under general anesthesia to assess efferent corticospinal motor tract integrity,[1] and somatosensory evoked potential (SEP) monitoring through the skull or brain surface to assess the activity of afferent peripheral nerves in the somatosensory tract.[9]

Electrophysiological techniques can establish neurological integrity, but are less useful for localizing eloquent areas within the surgical field that may be compromised during manipulation and result in postoperative functional impairments. Recently, techniques were described that allow the use of conventional bipolar forceps to function as stimulation electrodes.[6,11] However, this bipolar forceps is a dedicated probe for stimulation and must be exchanged for the coagulation forceps once the stimulation is complete.

Here we describe a novel surgical system (three-way bipolar forceps system) that integrates the functions of electrophysiological assessment (nerve stimulation and elicitation of potentials) with the conventional bipolar forceps used for resection and coagulation.

Received June 16, 2005; Accepted August 29, 2005

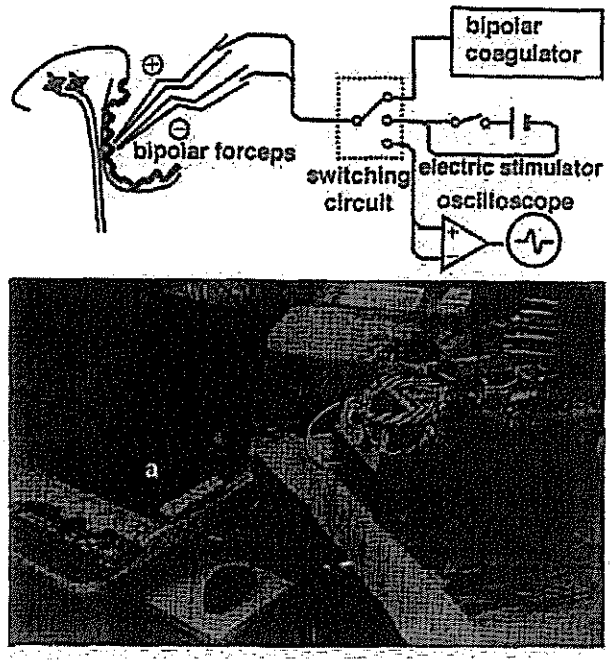

Fig. 1 *Upper*: **Schematic diagram of the three-way bipolar forceps system.** *Lower*: **Photograph of the system with electric stimulator (a), bipolar coagulator (b), and three-way switching circuit (c).**

Materials and Methods

I. Configuration of the three-way bipolar forceps system

A mechanical rotary switch (TS-2; Nihon Kaiheiki Industry Co., Ltd., Kawasaki, Kanagawa) was used as a switching device to control the flow of the electric current based on the desired function of the system (e.g., surgical manipulation vs. monitoring device). Device connectors were installed on a glass epoxy resin panel with a dielectric strength of 6 kV or more, and the connectors were linked with the devices using silicone-coated wire with a dielectric strength of 6 kV (AWG#14; Kyouwa Denko, Tokyo) (Fig. 1).

The switching circuit system was designed to provide an exclusive closed circuit to each modality, which consisted of the following components: a bipolar electrosurgery system (Micro-3 plus; Mizuho Ikakogyo Co., Ltd., Tokyo or MALIS CMC-II System; Codman & Shurtleff Inc., Raynham, Mass., U.S.A.), an electrical stimulator (Neuropack; Nihon Kohden, Tokyo or Ojemann cortical stimulator, OCS-1; Radionics, Burlington, Mass., U.S.A.), an amplifier (Neuropack), the mechanical rotary switch, and the connecting wire. The Neuropack is a system for the measurement of evoked potentials under general anesthesia and includes a built-in amplifier and an electrical stimulator. During awake surgery, the Ojemann cortical stimulator was used for functional mapping without an amplifier. The choice of the Neuropack or Ojemann stimulator was based on the location of the lesion and the surgical procedure. If stimulators were used simultaneously, one of the stimulators was always isolated from the three-way bipolar forceps system.

Each modality (bipolar electrosurgery system, amplifier, and electrical stimulator) was insulated to ensure safe surgery. Inputs and outputs were conducted through the patient's body using the conventional bipolar forceps as a mutual probe. The panel and the connecting wire had a dielectric strength of 6 kV or more, so the surgeons and operators responsible for operating the mechanical rotary switch were insulated appropriately to prevent electric shock. Therefore, the mechanical rotary switch was suitable for use under the varied electrical characteristics of different types of surgical devices as follows: coagulation (frequency, 1–5 MHz; amplitude, 300 Vpp; current, 500–1000 mA), nerve stimulation (1–50 Hz; 350 Vpp; 1–10 mA), and elicitation of nerve potential (5–10 kHz; 1 μ–10 mVpp; <1 mA).

The three-way bipolar system included a failsafe mechanism by which accidental use of a foot pedal could not cause coagulation if the device was set in the stimulation or elicitation mode. According to international standards for medical devices,[3,4] both dielectric strength and high frequency leakage current were measured on the three-way bipolar system connected with the bipolar electrosurgery system, the electrical stimulator, and the amplifier.

II. Measurement of forceps movement time

To evaluate the performance of the three-way bipolar system, the movement time between coagulation and stimulation was compared with the changing and movement time of a conventional bipolar forceps and conventional stimulator probe. Five neurosurgeons (mean age ± standard deviation, 37.4 ± 8.5 years), who were accustomed to handling the conventional bipolar forceps and the Ojemann stimulator, participated in this experiment.

For these experiments, small copper plates (3 × 3 mm) were arranged in a triangle (A, B, and C) on a circular silicone board (70 mm in diameter). Each apex consisted of two copper plates placed side-by-side to produce a short circuit when touched with the bipolar forceps or stimulator. Using the conventional or novel device, neurosurgeons were instruct-

ed to touch the three points (A, B, and C in this order) using the bipolar forceps (points A and C) or the stimulator probe (point B) under a stereoscopic microscope (×8) (AS-3; Nagashima Medical Instruments, Co., Ltd., Tokyo). The conventional bipolar forceps was held on point A for a given time, and then the tool was exchanged to the stimulator probe and moved to the next point B. The time from tool removal from point A and placement to point B was recorded. In contrast to the novel device, the surgeon was required to exchange the conventional bipolar forceps for a stimulator probe when using the conventional device. Next, the time from the stimulator probe removal of point B to the conventional bipolar forceps placement on point C was recorded.

Each neurosurgeon was allowed three practice runs to touch targets A, B, and C, one after another (e.g., A, B, C, A, B, C, A, B, and C in this order) using the tips of the forceps. Experimental determination of moving time was conducted with 10 trials for each neurosurgeon, and movement time (including changing time in case of conventional method) was measured. The measurements are expressed as mean ± standard deviation. Differences between means in moving time between the conventional and three-way bipolar forceps method were assessed by two-way repeated-measures analysis of variance.

III. Animal experiment

An animal experiment (4-month-old pig; body weight, 40 kg) was conducted to determine whether the electrical current flow can be safely switched. MEPs were measured continuously from the gastrocnemius muscle, and the left central sulcus to lateral ventricle was incised with simultaneous monitoring of the electrocardiogram and respiratory movement. The animal was anesthetized with intravenous administration of propofol (12 mg/kg/hr) (Diprivan; Astra Zeneca, London, U.K.), and needle electrodes were inserted in the gastrocnemius according to the belly-tendon method. After opening the dura mater, the motor area was electrically stimulated using the bipolar forceps connected to the switching circuit system. Stimulation was conducted with 5 train pulses of duration 0.2 msec and interstimulus interval of 2 msec with a stimulation intensity of 10 to 15 mA. The amplifier settings of the evoked potential-measuring system for the MEP were as follows: sensitivity, 50 μV/dlv; low-cut filter, 10 Hz; high-cut filter, 10 kHz.

IV. Clinical application

The bipolar electrosurgery system, the input terminal of evoked potential-measuring system, and the stimulator were connected to the exchange device. The operator changed the rotary switch to provide the functions of coagulation, electric stimulation, or SEP measurement upon request of the surgeon.

Ten patients with glioma underwent electrophysiological measurement of neuronal function by the three-way bipolar system during surgical resection of the tumor. Eight patients underwent awake craniotomy (frontal, n = 5; temporal, n = 2; occipital, n = 1), one patient underwent surgery (parietal) under general anesthesia, and the remaining patient also underwent surgery under general anesthesia. Written informed consent was obtained from all patients.

The performance of the three-way bipolar forceps was evaluated by functional mapping in the eight cases of awake craniotomy. Using the forceps, a mapping study (duration, 0.2 msec; stimulation intensity, 2 to 10 mA; stimulation frequency, 50 Hz) was conducted by monitoring the patient's movement and speech response to identify any eloquent areas within the surgical field.

SEPs were measured by stimulating (duration, 0.2 msec; intensity, 10 mA; frequency, 2.2 Hz) the left median nerve in one patient treated under general anesthesia. First, single channel SEPs were led from the scalp electrode attached to the C4', using Fz as a reference electrode. Next, two channel cortical SEPs were monitored using a strip electrode with four contacts (T-WS-4P; Ad-Tech Medical Instrument Co., Racine, Wis., U.S.A.) inserted from the opening of the skull to the front inferior surface of the dura mater. The strip electrode was placed at a right angle to an imaginary line that reflected the central sulcus. Finally, single channel SEPs were led from the brain surface using the tips of the three-way bipolar forceps as the anode or cathode.

An optical tracking system (Polaris; Northern Digital Inc., Calgary, Canada) was used to verify the tip location of the three-way bipolar forceps using a reflection marker in one patient treated under general anesthesia. Magnetic resonance (MR) images acquired intraoperatively were registered in the navigation system (Toshiba Medical Co., Ltd., Tokyo).[12] When the cortical and subcortical SEPs were monitored by stimulating the median nerve, the tip locations of the forceps for SEP elicitation were superimposed onto the registered MR images in three dimensions (sagittal, axial, and coronal way) and displayed on the monitor screen of the tracking system.[2]

Results

After the three modalities were connected to the

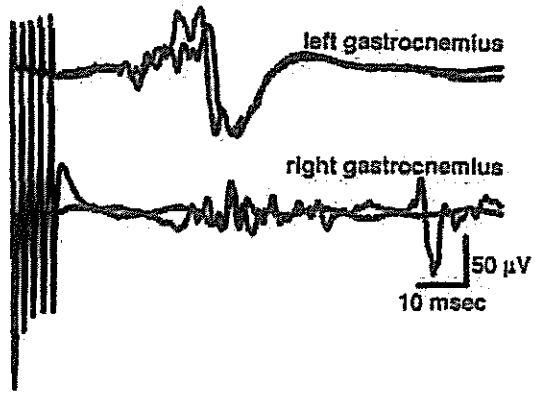

Fig. 2 Motor evoked potentials elicited from the pig lower limb by direct stimulation of the cortex using the three-way bipolar forceps.

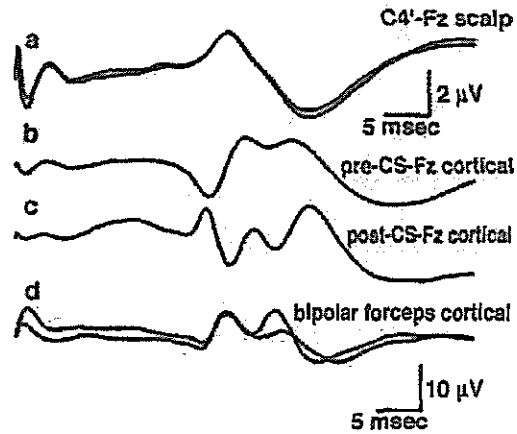

Fig. 3 Somatosensory evoked potentials (SEPs) obtained from a patient with left occipital glioma under general anesthesia. Traces in *a* represent ordinary SEPs elicited with the scalp electrode. Traces in *b* and *c* represent simultaneously measured SEPs from subdural cortical electrodes showing phase reversal waves as a result of placement of the two electrodes on opposite sides of the central sulcus. Traces in *d* are leading SEPs recorded with bipolar forceps. Traces in *b*, *c*, and *d* have the same calibration (10 μV).

three-way bipolar system, the dielectric strength between the forceps and the ground remained above the minimum voltage of each device.[3] The leakage current from the tips of the forceps to the ground was below the limit of the standard, when the switch position was set to the stimulator or the amplifier. Moreover, the high frequency leakage current between the forceps tips, which were switched to the electrical stimulator or the amplifier in faulty coagulation mode, was 18 mA, less than the calculated limit of 25 mA in the standard.[4]

The time duration between coagulation and stimulation was significantly shorter for the three-way bipolar system (1.12 ± 0.42 sec) than for the conventional procedure (3.63 ± 1.00 sec).

Use of the three-way bipolar forceps in the animal experiment verified that the apparatus could serve as a stimulation electrode as well as a coagulation device. Further, the switching procedure was performed safely without complication. Figure 2 shows the MEP recording from the porcine lower limbs by cortex stimulation with the three-way bipolar forceps. The onset latency (left, 20 to 23 msec; right, 33 to 39 msec) and the amplitude (left, 20 to 120 μV; right, 30 to 50 μV) varied in each trial.

In patients undergoing awake craniotomy, the functional area was successfully identified by functional mapping using the stimulation function of the three-way bipolar forceps. Figure 3 depicts the SEP recording of one patient under general anesthesia. The wave profile of the strip electrode and the three-way bipolar forceps used to identify the central sulcus were somewhat larger than that obtained via the scalp electrodes. With the disk electrode, 200 stimulations were required to obtain a reproducible wave profile of SEPs (peak latency, 22 msec; amplitude, 3.5 μV) (Fig. 3 *a*). In the wave profile of the cortical SEPs (Fig. 3 *b* and *c*) measured using the strip electrode, a phase reversal was observed between two traces obtained from neighboring two contacts. Consequently, the two contacts of the strip electrode were confirmed to be placed behind and in front of the central sulcus. With the strip electrode, 80 stimulations were required to generate reproducible SEPs (peak latency, 20 msec; amplitude, 12 μV). With the three-way bipolar forceps, 60 stimulations were sufficient to obtain a steady wave profile of SEPs (peak latency, 22 msec; amplitude, 11 μV).

When the navigation system was used, the optical marker placed on the tip of the three-way forceps disclosed that the sensory area overlapped with a portion of the surgical field (Fig. 4). The three-way bipolar forceps could induce the subcortical SEPs (Fig. 4 *b*) after tumor resection as well as the cortical SEP (Fig. 4 *a*).

Discussion

The present study demonstrated that use of the three-way bipolar forceps reduced the time required to achieve two of the three actions (coagulation, electrical stimulation, and elicitation) and can facilitate neurosurgical procedures. The time measurement reflects the correctness of the probe

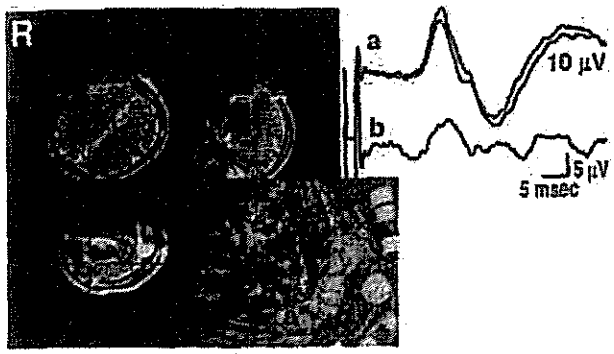

Fig. 4 Navigation of three-way bipolar forceps superimposed on intraoperative magnetic resonance images of a patient with right parietal glioma. Somatosensory evoked potential (SEP) traces in *a* and *b* correspond to positions *a and *b** on the surface image of the brain cortex. Virtual needle on the navigation image shows the location of the bipolar forceps eliciting the SEP in *b*.**

position with tool exchange. The three-way bipolar system can maintain the accuracy of probe location during coagulation, stimulation, and elicitation. The benefit of this system may be even greater if the region to be manipulated is close to the eloquent areas. The frequency of interruptions in the surgical procedure by changing tools may stress the neurosurgeon. For examples, in one case of vestibular schwannoma, 34 exchanges (total 29 min) were required using conventional devices within a 9-hour surgery (data not shown). Although stimulation required less than 1 minute, repetition of the exchange action resulted in a significantly longer operative time.

In the animal experiment, MEPs were observed in the lower limbs after electrical stimulation using the three-way bipolar forceps as an electrode. MEPs elicited by direct stimulation onto the motor cortex can locally stimulate the motor area.[5] In the present study, the three-way bipolar forceps could induce micro-stimulation of the motor nerve. This observation suggests that functional mapping can be achieved without changing the instruments, so simplifying the surgical procedure and reducing operative time.

This novel system could perform functional mapping during awake craniotomy equivalent to that achieved by the Ojemann cortical stimulator probe. After confirmation of the safety, the three-way bipolar system can be used for MEP measurement by stimulation of the deep brain, where frequent exchanges between the stimulator probe and the bipolar forceps are necessary and a shift of a few millimeters in the location of coagulation affects the functional outcome. The stimulation time required to achieve a stable SEP profile was shorter with the three-way bipolar forceps (60 stimulations) compared with the disk electrode (200 stimulations) or the strip electrode (80 stimulations), which suggests that the three-way bipolar forceps has the highest signal-to-noise ratio. Thus, this system can elicit evoked potentials from a limited locus in approximately one-third the time required for a similar function to be achieved by ordinary SEP from scalp electrodes due to the lower common-mode noise ratio. However, there are differences in the electrode distance between anode and cathode between the two systems, resulting in slightly different SEP elicitation. Thus, interpretation of the wave profile requires caution.[6]

Tissue commonly sticks to the tip of the bipolar forceps due to carbonization of coagulated tissue, resulting in increased resistance to current flow. The standards for surgical equipment require the load resistance for the bipolar outputs to be between 10 ohm and 1 kohm.[4] Therefore, the bipolar surgical system should allow normal coagulation with 1 kohm resistance between the tips. The specification of the load resistance of electrical stimulator (Neuropack) is also 1 kohm. Even with coagulated tissue attached to the tip of the bipolar forceps at 1 kohm resistance, constant current electrical stimulation will be delivered normally. However, the input resistance of the amplifier is 200 Mohm. Therefore, 1 kohm contact resistance on the bipolar tips will scarcely distort (only 1/200001 decrease will occur) the SEP waveforms. The bipolar system, MALIS CMC-II System, is used together with a saline irrigation system. Therefore, both stimulation and elicitation will not be so much affected by the coagulated tissue except for the carbonized tips which can no longer coagulate tissue.

Considering the electrical charge effect on the forceps tips after each modality, the coagulation current will not cause polarization because of the characteristics of alternating current. The electrical stimulations are bipolar, so each tip will act as the anode or cathode. Such polarization will disappear through tissue contact resistance (as much as 1 kohm) within a few seconds. Therefore, SEP measurement after electrical stimulation will not be affected by the polarization.

The three-way bipolar forceps system has multiple functions, including hemostasis, coagulation, nerve stimulation, and elicitation of potentials. Further, this integrated system is technically easy to operate and allows functional monitoring of an area that would otherwise be difficult to perform using con-